46th AIAA Aerospace Sciences Meeting and Exhibit
7 - 10 January 2008, Reno, Nevada

AIAA 2008-1047

Three-dimensional Numerical Simulation of Flames Supported by a Spinning Porous Plug Burner

Kishwar N. Hossain* and Thomas L. Jackson †
University of Illinois, Urbana, IL 61801

John D. Buckmaster‡
Buckmaster Research, Urbana, IL, 61801

A three-dimensional numerical study is undertaken to analyze the characteristics of flames supported by a spinning porous plug methane burner. These flames are characterized by multi-dimensional instabilities at near extinction conditions. The instabilities appear in the form of holes and spirals as observed in experimental studies,[1,2] The non-uniform flames are simulated numerically for Damköhler numbers on the upper branch of the S-response curve close to the extinction point. The flames are analyzed to determine the mechanism of onset of the patterns and to gain an understanding of the dynamics of the system.

I. Introduction

The evolution of non-uniform flames is typically a manifestation of the intrinsic instabilities of the system. These instabilities lead to dynamics that are unique and offer insight into the conditions necessary for the sustainability of the flame. An understanding of these instabilities can also be of importance to turbulence modeling. The flame supported by a rotating porous plug burner offers a suitable platform for the study of such an instability. Here the non-uniformity appears in the form of flame holes and spirals. The spirals are particularly interesting because they are distinct flames that rotate about the axis of the burner, and thus simultaneously support an ignition front and a trailing extinction front. This study aims to identify the conditions that render the diffusion flame formed on a rotating porous plug burner unstable, and to analyze the features of the resulting non-uniform flame such as the dynamic edges, the characteristics of which may be of some importance to the study of turbulent flames. We begin our discussion with a more detailed look at the configuration we are considering and a review of other studies that provide information on the onset of instabilities in diffusion flames.

Rotation of the porous plug causes a flow of the ambient air toward the burner, while there is a steady flow of fuel from the burner exit. Consequently, the fuel and air mix at a finite distance above the burner surface and a diffusion flame is formed. Here, the injection velocity of the fuel is w_0 and the angular velocity of the burner is b_0. If $b_0 > 0$ then the burner rotates counterclockwise. In this study the fuel is taken to be methane and the oxidizer is air. The viscosity, thermal conductivity, and the specific heat at constant pressure are taken to be constants. The density is also taken to be constant, uncoupling the mass and momentum equations from the energy and species equations. The flow is solved, independently of the combustion equations, using the similarity solution for the Von Karman swirling flow. For the combustion equations, a one-step global irreversible reaction is considered and the reaction rate is taken to be of the Arrhenius type. The system of unsteady, three-dimensional equations is then solved numerically using the velocity profiles as inputs.

Experimental studies using the rotating burner configuration show the evolution of non-uniform flames with variations in the rotational speeds of the burner,[1,2] At low rotational speeds a steady flat flame is observed. As the rotational

*Graduate Student, Department of Aerospace Engineering, University of Illinois, Urbana, IL, Student Member
†Senior Research Scientist, Center for Simulation of Advanced Rockets, University of Illinois, Urbana, IL, Associate Fellow, AIAA, Corresponding Author, tlj@uiuc.edu.
‡Buckmaster Research, Urbana, IL, Associate Fellow, AIAA

speed is increased pulsating flame holes, single armed spirals and eventually multiarmed spirals are observed. A related asymptotic study, by Nayagam and Williams,[3] on inflammability limits of a stagnation point flow impinging on a spinning fuel disk, shows that the inflammability boundaries for the one-dimensional system are a function of the strain-rate parameter.

The influence of the strain-rate on the stability of diffusion flames is also evidenced in a study of flames formed between opposed slot jet burners[4] where there exists a threshold for the local strain-rate value below which the spatially uniform diffusion flame is replaced by a stable edge flame configuration. These destabilizing effects of the strain rate on diffusion flames are typically a transitional state between the fast time stable, and unstable branches of the S-shaped response curve which depicts the maximum temperature as a function of a Damköhler number, which is typically a function of the strain rate. In experimental studies of non-premixed flames oscillations and cellular flames are generally observed at near extinction Damköhler numbers,[5,6] Theoretical studies by Cheatham and Matalon,[7] and by Kukuck and Matalon[8] also reverberate this notion.

The experimental study of flame holes by Pellet et al.[9] shows that increases in the flow velocities cause a disk flame to "rupture" from the center outward. A reduction of the mass flow rate following the "rupture" leads to a shrinking and shifting of the ring until the disk flame is restored. A subsequent two-dimensional numerical study of Frouzakis et al.,[10] reproduces the qualitative results of Pellet et al., and shows that an increase in the Reynolds number of the flow leads to the local extinction of the flat diffusion flame and the formation of an edge-flame. In another two-dimensional numerical study, Lu and Ghoshal[11] show that the dynamic behavior of a hole is dependent on the strain rate and the hole radius; for every strain rate there is a critical hole radius that is a bifurcation point and separates the expanding and shrinking behavior. Buckmaster and Jackson,[12] in their investigation of the propensity of holes to close in a zero velocity field, identify a detachment Damköhler number, the maximum Damköhler number for which a hole will expand.

Although the onset of instability is typically a function of the Damköhler number, there are other parameters that affect it as well. Theoretical studies by Kukuck and Matalon,[8] and Short and Lui[13] show that wall boundary conditions, namely the mixture strength and the fuel supply temperature, have a significant effect on the range of Damköhler numbers within which the system becomes unstable. Heat losses to the channel walls also have an effect on the stability of the system. The effect of heat loss is considered in detail in the context of a premixed flame anchored to a porous plug burner by Margolis[14] and by Buckmaster.[15] These studies show that heat loss to the burner has a stabilizing effect on the left stability boundary of the premixed flame. In terms of the right stability boundary, increases in the heat loss lead to a destabilizing shift till a threshold is reached, beyond which the burner is stabilizing. For high enough values of the activation energy, a Lewis number stability band does not exist.

The focus of this paper is to summarize results of a three-dimensional numerical investigation of the near extinction behavior of flames supported by a spinning methane burner. The range of Damköhler numbers within which non-uniform flames, qualitatively similar to those observed by Nayagam and Williams,[1] can be sustained is identified. Following is a detailed account of the formulation in and a discussion of the numerical method in section II, and a discussion of the results is given in section III.

II. Non-dimensional Equations and Solution Methodology

For non-dimensionalization, the lengths are scaled by $\sqrt{\nu/b_0}$, time by the reciprocal of b_0, temperature by T_∞, and the species by Y_{f0}, the mass fraction of the fuel at the burner exit. The similarity variables for the velocities are

$$F = u/(b_0 r), \quad G = v/(b_0 r), \quad H = w/\sqrt{b_0 \nu}, \tag{1}$$

where F, G, H are functions of z. The resulting non-dimensional equations are

$$H' = -2F, \quad F'' = F^2 + F'H - G^2,$$

$$G'' = 2FG + HG'. \tag{2}$$

The appropriate boundary conditions are

$$F(0) = 0, \quad G(0) = 1, \quad H(0) = H_0,$$
$$F(\infty) = 0, \quad G(\infty) = 0. \tag{3}$$

The non-dimensional unsteady energy and species equations are given by

$$L[T, Y_i] - M[T, Le_i Y_i] = \Omega[\beta, -\alpha_i], \tag{4}$$

where

$$\mathbf{L} = \partial/\partial t + rF\partial/\partial r + G\partial/\partial\theta + H\partial/\partial z,$$
$$\mathbf{M} = r^{-1}\,\partial/\partial r + \partial^2/\partial r^2 + r^{-2}\,\partial^2/\partial\theta^2 + \partial^2/\partial z^2.$$

Here, $Le_i = \rho C_p D_i/\lambda$, is the Lewis number for species i, $\beta = QY_{f0}/C_pT_0$, the heat release parameter, $\Omega = D\overline{D}Y_oY_f exp\{Ze(1 - T^*/T)\}$, the reaction rate, $D = Bb_0^{-1}\rho^{-1}Y_{f0}$, the Damköhler number, $Z_e = E/(R_uT_0T^*)$ the Zeldovich number, $\overline{D} = Ze^3T^*/z^{*2}$, a scaling factor, and, T^* and z^* the Burke-Schumann flame temperature and flame location, respectively, for the baseline parameters listed in section III.A. The Prandtl number, $Pr = \nu\rho C_p/\lambda$, is set to 1.0. The boundary conditions are

$$\begin{aligned}
z = 0: &\qquad T_0 = T_s,\ \ Y_{f_z} = H_0 Le_f(Y_f - 1),\\
&\qquad Y_{o_z} = H_0 Le_o Y_o,\\
z = \infty: &\qquad T_\infty = 1,\ \ Y_f = 0,\ \ Y_o = \phi^{-1},\\
r = 0: &\qquad T_r = 0,\ \ Y_{i_r} = 0,\\
r = \infty: &\qquad T_r = 0,\ \ Y_{i_r} = 0,
\end{aligned}$$

and periodic in θ

$$T_\theta|_{\theta=0} = T_\theta|_{\theta=2\pi},\ \ Y_{i_\theta}|_{\theta=0} = Y_{i_\theta}|_{\theta=2\pi},$$
$$T_\theta|_{\theta=0} = T_\theta|_{\theta=2\pi},\ \ Y_{i_\theta}|_{\theta=0} = Y_{i_\theta}|_{\theta=2\pi}.$$

Here, ϕ is the mixture strength defined as the ratio of the fuel mass fraction at the burner surface to the oxidizer mass fraction at infinity. This definition of the mixture strength is not normalized by the stoichiometric coefficients and is thus different from the one used by Kukuck and Matalon.[8] At the burner surface the non-dimensional temperature is set to a constant, T_s, and at $z = \infty$ the temperature is set to the ambient temperature, unity, while the fuel mass fraction is set to zero. Neumann boundary conditions are applied at the radial boundaries, while the temperature and species are taken to be periodic in θ . For the current study the fuel is taken to be methane, and the oxidizer is air; thus, $Le_f = 1.0$, $Le_o = 1.0$, $\alpha_f = 0.25$ and $\alpha_o = 1.0$. The mass fraction of air at infinity, $Y_{o\infty}$ is taken to be 0.2. The parameters of study are D, T_s, H_0, and ϕ. β is adjusted to fix the Burke-Schumann flame temperature while Ze is kept constant. The one-dimensional similarity equations of the Von Karman spinning disk flow, given by equation (2), are solved using the COLSYS package.[16] The energy and species equations, (4), are solved using a fourth-order centered finite difference scheme in space and a $2N$-storage, five-stage, fourth-order Runge-Kutta scheme, $(5, 4)\ RK$, in time.[17] The computations are performed on parallel processors using the MPI protocol. The simulation results are obtained using a 64 cubed grid which proved to be sufficient in a convergence study. The simulations commence at large Damköhler numbers where the fast chemistry limit is valid, and so the Burke-Schumann flame sheet solution is used as the initial condition. Radial and angular perturbations are introduced once steady-state is reached for a given Damköhler number. If the perturbations do not result in sustainable instabilities the simulations are restarted at a lower Damköhler number using the steady-state solution from the previous Damköhler number as the initial condition. This process is repeated till the non-uniform flames appear.

III. Results

III.A. The Burke-Schumann Flame Sheet

The Burke-Schumann limit is important to consider in order to gain a fundamental understanding of the diffusion flame, and to establish initial conditions for numerical solutions. This limit arises as $D \to \infty$ resulting in an infinite reaction rate that can be balanced by taking the flame sheet to be very thin such that $Y_f Y_0 \to 0$. This thin flat flame sheet forms at a distance z^* from the burner surface and separates the fuel and the oxidizer. At this limit the combustion field is expected to be a function of z and t only and the temperature and species profiles are given by

$$\begin{aligned} 0 < z < z^* : \qquad & T = Z_+, \;\; Y_o = 0, \\ & Y_f = \beta^{-1}\alpha_f(Z_- - Z_+), \end{aligned}$$

and

$$\begin{aligned} z^* < z < z_\infty : \qquad & T = Z_-, \;\; Y_f = 0, \\ & Y_o = \beta^{-1}\alpha_o(Z_+ - Z_-), \end{aligned} \tag{5}$$

where the Schvab-Zeldovich variables are

$$Z_+ = T + \beta\alpha_f^{-1}Y_f \;\text{ and }\; Z_- = T + \beta\alpha_o^{-1}Y_o \tag{6}$$

and the matching condition

$$Z_+(z^*) = Z_-(z^*) \tag{7}$$

is used to determine z^*. The steady state solutions for Z_+ and Z_- are obtained using COLSYS. For $H_0 = 0.1$, $T_s = 1.0$, $\phi = 2.0$, $\beta = 25.0$ and $Ze = 40$, the baseline parameters for this study denoted as Case 1, the Burke-Schumann flame temperature is $T^* = 7.43$, and the flame location is $z^* = 1.54$. These values of the flame temperature and flame location are used in section II in the scaling factor for the Damköhler number.

III.B. Three-dimensional Simulations

The stability of the three-dimensional spinning burner configuration is investigated using small pure mode perturbations. It is found that at appropriate Damköhler numbers these perturbations result in non-uniform flame patterns such as holes and spirals. This phenomenon is first investigated for parameter values listed in the previous section for Case 1. Figures 1 and 2 show the velocity profiles and the S-shaped response curve, respectively, for this set of parameters. The extinction point, D_E, is approximately 1.48 as seen from figure 2. $D^* = 1.96$ represents the highest Damköhler number at which sustainable non-uniform flames appear. As seen from figure 2 the range of Damköhler numbers within which these non-uniform flames appear is small. However, this range can be further divided into smaller intervals where different modes are viable. For example, for the set of parameters listed above, the flame hole first appears at $D = 1.96$, the single spirals at $D = 1.91$ while the double spiral appears first at $D = 1.85$. It is expected that as the Damköhler number is lowered the ranges within which higher modes are sustained can be determined. However, for this section the discussion is limited up to double spirals, primarily due to the fact that for the higher modes the ranges become smaller and so it is difficult to identify distinct regions corresponding to each mode. The progression of the flames from the flame hole to the single armed and then the multiarmed spirals with decreasing Damköhler number is reminiscent of the observations of Nayagam and Williams[2] where the flames transition from flame holes to spirals with increasing angular velocity. It should be noted that in the current formulation the Damköhler number is inversely proportional to the angular velocity. Thus the trends observed in the simulations are similar to those found in the experimental studies.

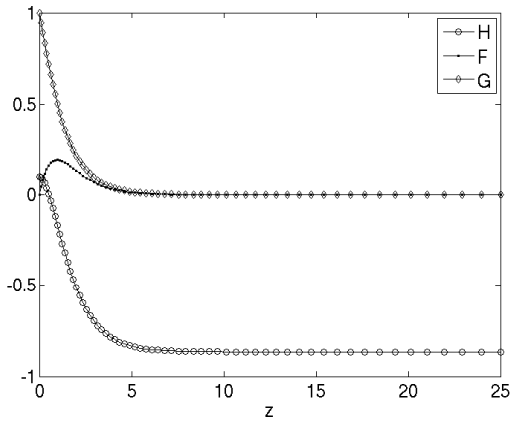

Figure 1: Non-dimensional Velocities.

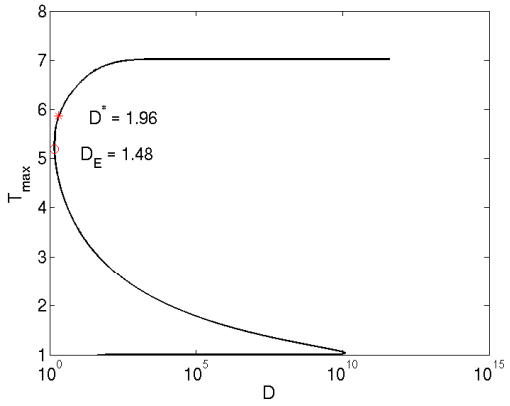

Figure 2: S-shaped Response Curve.

III.C. Flame Hole

Figure 3 shows the temperature contours in the xy-plane of a flame hole at $D = 1.96$ at the stoichiometric height. Here, a central cold region is surrounded by an axisymmetric, annular flame sheet. A region of high temperature appears immediately adjacent to the boundary of the flame hole and then the temperature gradually decreases and oscillates along the radius as shown in figure 4. The geometry of the flame hole is better illustrated in the temperature contour in the rz plane given in figure 5. The edge of the flame is at a radial location of approximately $r = 13.4$. There is a region of high temperature adjacent to the flame edge, trailed by a lower temperature flame till the outer radial boundary. Additional information about the flame is obtained from the cross-scalar dissipation contours shown in figure 6, defined as

$$\chi_c = \nabla Y_f \cdot \nabla Y_o. \tag{8}$$

The cross-scalar dissipation rate is negative for diffusion flames and positive for premixed flames.[18] As seen from this figure there is some premixing near the location of the edge of the flame hole. The high temperatures in the triangular region adjacent to the flame hole could be attributed to this premixing. This figure also indicates that the tail of the annular flame is purely diffusional.

The radial oscillations in the trailing diffusion flame beyond the hole region are visible in the rz contours as well. These oscillations can be explained by considering small perturbations in the large z field. As $z \to \infty$ the angular and radial velocities become negligible while the axial velocity asymptotes to H_∞. Here, the solution of the homogeneous

heat equation is given by

$$T = exp(-1/2[H_\infty + \sqrt{H_\infty^2 + 4\mu^2}]z)J_0(\mu r). \tag{9}$$

It is found that the wavelength of the radial oscillations shown in figure 4 correspond to $\mu \approx 0.14$ which implies

$$T = exp(H_\infty z)J_0(\mu r) \tag{10}$$

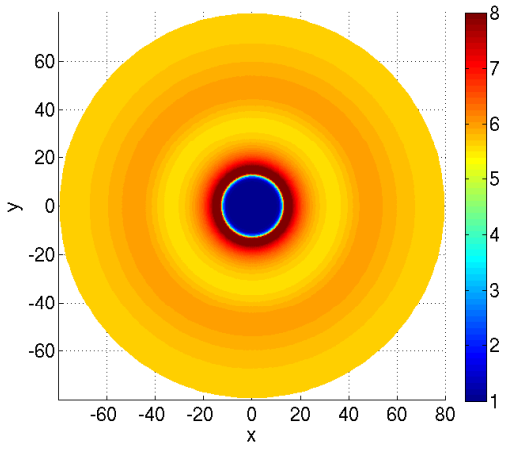

Figure 3: Flame Hole for Case 1, $D = 1.96$.

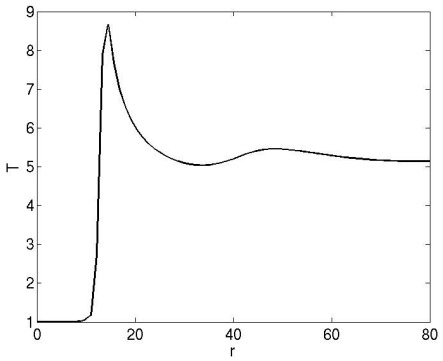

Figure 4: Radial Temperature Profile at $\theta = 0rad$.

III.D. Effect of Damköhler Number on Flame Hole Radius

The flame hole is the first non-uniform flame observed as the value of the Damköhler number nears the extinction value, D_E. The flame hole forms at a Damköhler number of 1.96 while a single spiral forms at $D = 1.9$. It is found that at Damköhler numbers between these two values the flame hole expands with decreasing Damköhler number. Flame holes are simulated for $1.940 \leq D \leq 1.960$ and the flame hole radii, defined as the distance from the axis to the point where the temperature rises above 5 in the stoichiometric plane, are tabulated in table 1. As seen from this table there is a significant increase in the flame hole radius within the range of Damköhler numbers considered. Another point of note is that the radii of the flame holes are large and so the concept of edge speeds is probably appropriate. Although the flame holes have stationary edges, it should be noted that these edges are stationary relative to a non-zero

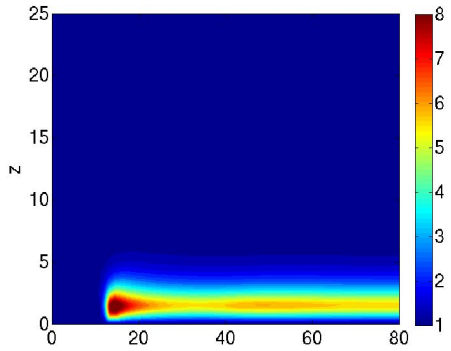

Figure 5: Temperature Contour in the rz Plane of a Flame Hole for Case 1, $D = 1.96$.

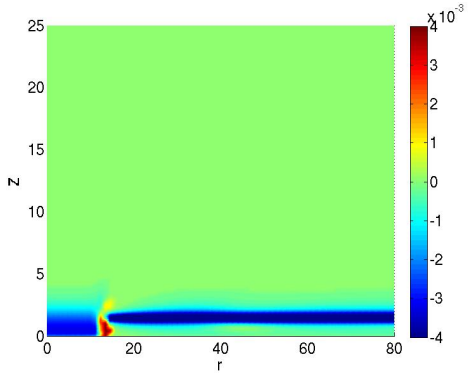

Figure 6: Cross-Scalar Dissipation Contour in the rz Plane of a Flame Hole for Case 1, $D = 1.96$.

D	Hole Radius	Temp (r=80)	1-D Flame Temp
1.960	13.37	5.54	5.857
1.955	20.35	5.61	5.857
1.950	22.73	5.40	5.857
1.945	31.24	5.87	5.857
1.940	34.97	5.76	5.848

Table 1: Damköhler Number and Flame Hole Radii.

radial velocity that is a function of the radius at the stoichimetic height. Thus, an expansion of the flame hole suggests an increase in the edge speed with decreasing Damköhler number. The temperature contours in the rz plane suggest that the tail of the flame is purely diffusional and from table 1 it is seen that the temperatures at $r = 80$ are generally close to the flame sheet temperatures.

III.E. Single Spiral

Figure 7 shows the temperature and species contours for a single spiral for $D = 1.91$. The spiral rotates as a rigid body at a rate of $-0.14\ rad/time$, while the burner rotates at $b_0 = 1\ rad/time$ and at the stoichiometric height the angular velocity is $b = 0.45\ rad/time$. This high relative angular velocity is believed to be one of the main factors contributing to the differences in the characteristics of the leading edge as compared to the the trailing one. As seen

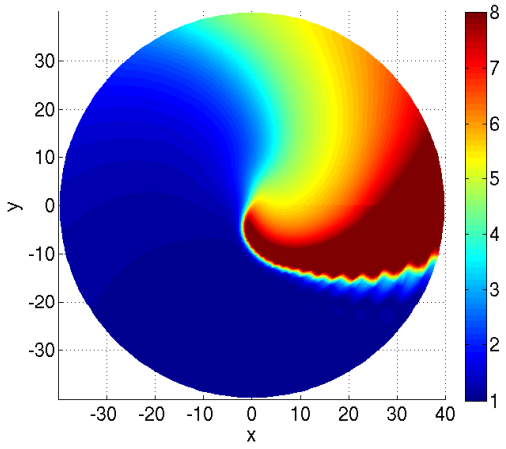

Figure 7: Single Spiral for Case 1, $D = 1.91$.

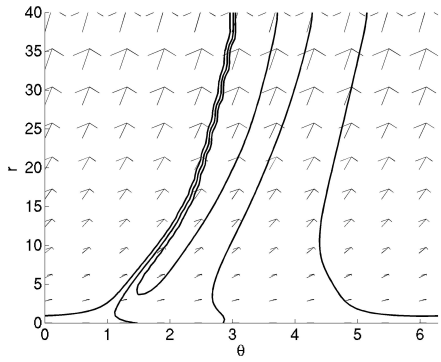

Figure 8: Single Spiral Contours and Relative Velocity Vectors for Case 1, $D = 1.91$. Contour Values:4, 6, 8.

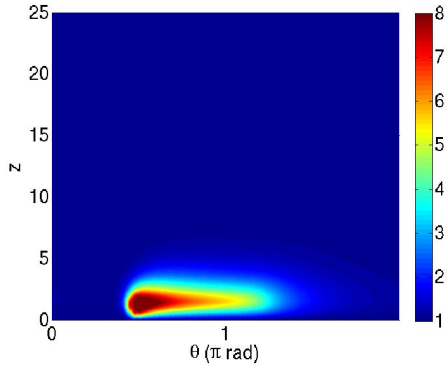

Figure 9: Single Spiral for Case 1 in the $z\theta$ plane, at $r = 40$, $D = 1.91$.

from figure 7 the temperature gradient is steep at the leading edge while there is a more gradual variation at the tail. This trend is similar to the one seen in the case of the flame hole where the stationary "leading edge" displays a high temperature gradient. Another point of note are the wiggles that are present at the leading edge of the spiral. These

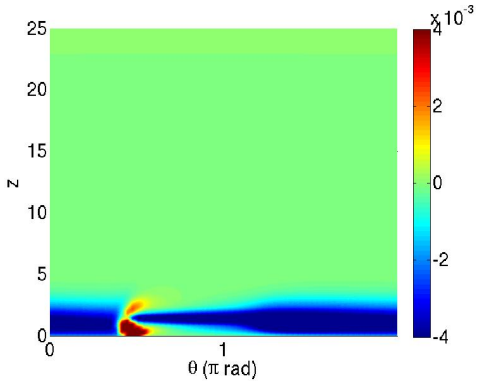

Figure 10: Cross Scalar Dissipation Contours of the Single Spiral for Case 1 at $r = 40$, $D = 1.91$.

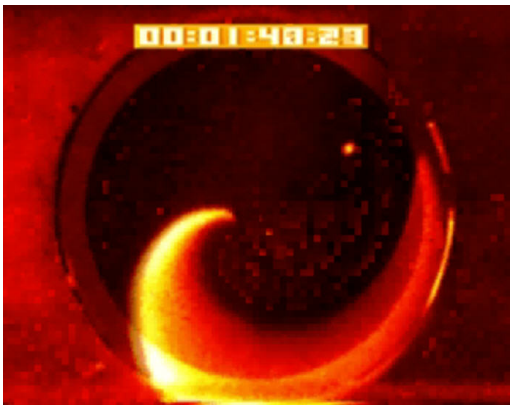

Figure 11: Single Spiral Observed in the Experiments of Nayagam and Williams (Printed with Permission).

oscillations arise due to difficulties in fully resolving the dynamic edge of the flame. It is found that increasing the grid density reduces the prominence of these oscillations, however, due to time constraints, the finer grid is not used.

The shape of the spiral is affected by the velocity field as well. In the $r\theta$ plane the temperature profile can be described as a wave that is advected in θ. The line connecting the peak temperatures of these waves at each r location is at an angle that can be approximated by the resultant of the radial and angular velocities. This is demonstrated in figure 8 where the velocity field is superimposed on the temperature contours. As seen here the velocity vectors are almost tangent to the temperature contours. It is also found that as the Damköhler number is reduced, there is no discernable effect on either the speed or the shape of the spiral. This indicates that, although the Damköhler number is responsible for triggering the instability, the dynamics and the geometry of the single spiral are primarily functions of the velocity field as represented by the similarity variables. Another point of note is that the tip of the flame is anchored to the axis of the burner and there is no discernable meandering.

Figure 9 shows the temperature contours of the single spiral in the $z\theta$ plane. The shape of the contours at the leading edge of the spiral is similar to the shape of the temperature contours adjacent to the hole region shown in figure 5. The cross-scalar dissipation rate contours shown in figure 10 show that there is some premixing near the leading edge of the flame. This explains the higher temperatures at this edge as compared to the tail.

The single spirals simulated in this study are qualitatively similar to the one observed in the experiments. A snapshot of one such spiral is shown in figure 11 (obtained in a private communication with Vedha Nayagam and printed with permission). This spiral rotates clockwise and the temperature gradients at the leading edge are steeper than those in the trailing one. One primary difference between the experimental results and the simulated ones is

the absence of tip meandering in the simulated spirals. This difference could be attributed to hydrodynamics effects which are ignored in the current study. However, the qualitative similarities between the experimental and numerical spirals suggest that the inception of these non-uniform flames is a result of thermo-diffusional instabilities although their propagation may be affected by changes in the flow field.

III.F. Double Spiral

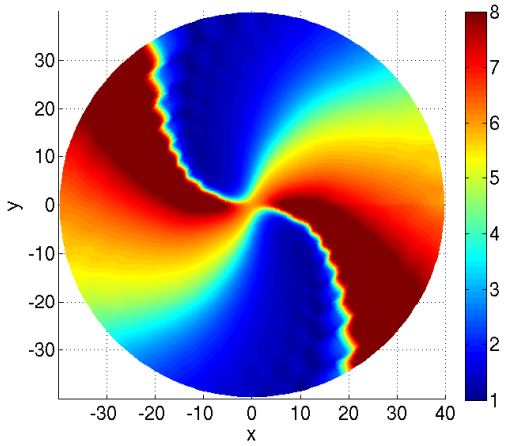

Figure 12: Double Spiral for Case 1, $D = 1.85$.

The double spiral shown in figure 12 is for $D = 1.85$ and rotates at $0.08\ rad/time$. As in the case of the single spiral, the leading edge of the flame relative to the flow, is the one with the steeper temperature gradients and the temperature contours in the $z\theta$ plane, as shown in figure 13. Also, each arm of the double spiral is similar in shape to the single spiral discussed in the previous section. However, in contrast to the single spiral, the double spiral rotates in the same direction as the burner, and the curvature of the leading edge is concave. These differences in the dynamics and the shape of the spirals in the xy plane is attributed to interactions between the two arms of the spiral as depicted in the temperature contours shown in figure 12, where some tip interaction is apparent. Interaction is also evident in the species contours in the $z\theta$ plane as shown in figures 14a and b. Thus, along with the Damköhler number and the velocity profile, interactions between the spirals also affect the shape and dynamics of these flames. Figure 15 shows

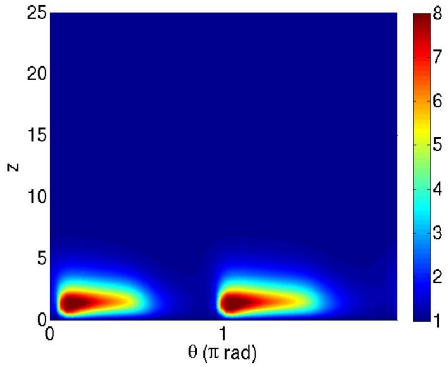

Figure 13: Temperature Contours for the Double Spirals in the $z\theta$ Plane for Case 1 at $r = 40$, $D = 1.85$.

the contours of the cross scalar dissipation rate for the double spirals. As seen here, the cross-scalar dissipation rate is

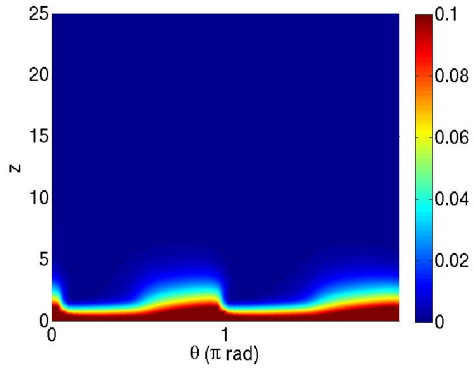

a. Y_f

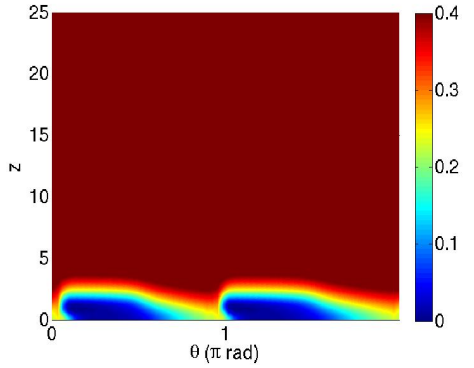

b. Y_o

Figure 14: Species Contours in the $z\theta$ Plane of a Double Spiral for Case 1 at $r = 40$, $D = 1.85$.

generally positive near the tip of the flame while it is negative in the tail. Thus, as in the cases of the flame hole and the single spiral some premixing occurs toward the front edges but most of the flame is primarily a diffusion flame.

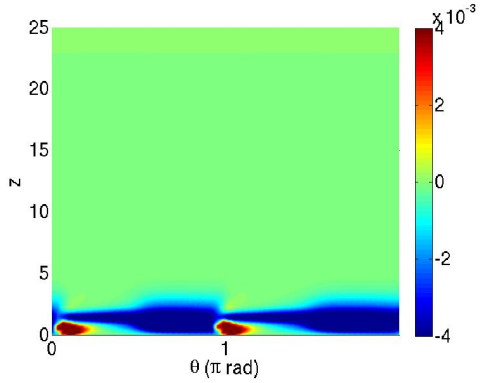

Figure 15: Cross Scalar Dissipation Contours for the Double Spirals for Case 1 at $r = 40$, $D = 1.85$.

III.G. Effect of Parameters of Study on the Stability of the System

In the previous sections it has been shown that the Damköhler number is the crucial paramter affecting the stability of the system. However, other factors such as the wall boundary conditions are also expected to have an effect, especially in terms of the range of Damköhler numbers within which non-uniform flames can be sustained. This is demonstrated in table 2 where the extinction Damköhler numbers are reported for four different parameter combinations. Here the heat release parameter is adjusted to fix the Burke-Schumann flame temperature. These values suggest that the injection velocity and the mixture strength have a considerable effect on the stability of the system while the effect of the temperature at the burner exit is small in comparison. Increasing the mixture strength leads to a shrinkage of the range whereas an increase in the injection velocity leads to an expansion. The trend in terms of the mixture strength is opposite to that observed by Kukuck and Matalon[8] for planar oscillations in diffusion flames. In the case of the spinning burner, an increase in the mixture strength leads to a shifting of the height of stoichiometry away from the burner surface to a region where the radial and angular velocities are lower in magnitude since the velocity profile remains unchanged. This reduction in the velocities in the vicinity of the flame sheet may have a stabilizing effect and so the Damköhler number range for instability is significantly reduced. An increase in the injection velocity, on the other hand, results in both a shift in the stoichiometric height and velocity profile. This dual change may be the cause of the expansion of the range.

Case	H_0	ϕ	T_s	D_E	D^*	D_E/D^*
1	0.10	2.0	1.0	1.48	1.96	0.76
2	0.10	2.0	1.4	1.46	1.95	0.75
3	0.10	5.0	1.0	1.78	1.87	0.95
4	0.05	5.0	1.0	5.25	6.32	0.83

Table 2: Effect of Parameters of Study on D^*.

IV. Conclusion and Future Work

In this paper a simple model is utilized to gain some insights into the stability of diffusion flames supported by a spinning porous plug methane burner. The evolution of the flame holes and spirals indicate that diffusion flames supported by the rotating porous plug burner become unstable at near extinction Damköhler numbers on the upper branch of the S-response curve. It is shown that these multidimensional instabilities are thermo-diffusional in nature. The flames have three-dimensional characteristics and the spirals are dynamic in nature. They rotate about the axis of the burner and the single-armed spiral rotates clockwise while the double-armed spiral rotates counter clockwise. The primary factors affecting the shape and dynamics of the spirals are identified as the velocity field and the interaction between spiral flamelets. It is also found that the mixture strength and the injection velocity have a significant effect on the range of Damköhler numbers within which the system is prone to instability.

Acknowledgments

This work was supported by the Center for Simulation of Advanced Rockets (CSAR) under contract number B523819 by the US Department of Energy as a part of its Advanced Simulation and Computing program (ASC). John Buckmaster was also supported by AFRL under grant number FA9550-05-1-0029, program manager Dr. A.Nachman..

References

[1]Nayagam, V. and Williams, F. A., "Pattern Formation in Diffusion Flames Embedded in Von Karman Swirling Flows," *NASA/CP 2001-21082*, 2001.

[2]Nayagam, V. and Williams, F. A., "Pattern Formation in Diffusion flames Embedded in Von Karman Swirling Flows," *NASA/CR 2006-*

214057, 2006.

[3]Nayagam, V. and Williams, F. A., "Diffusion Flame Extinction for a Spining Fuel Disk in an Oxidizer Counterflow," *Proceedings of the Combustion Institute*, Vol. 28, 2000, pp. 2875–2881.

[4]Shay, M. L. and Ronney, P. D., "Nonpremixed Edge Flames in Spatially Varying Straining Flows," *Combustion and Flame*, Vol. 112, 1998, pp. 117–180.

[5]Ishizuka, S. and Tsuji, H., "An Experimental Study of Effect of Inert Gases on Extinction of Laminar Diffusion Flames," *Eighteenth Symposium (International) on Combustion*, 1981, pp. 695–703.

[6]Chen, R., Mitchell, B. G., and Ronney, P. D., "Diffusive-Thermal Instability and Flame Extinction in Nonpremixed Combustion," *Twenty-fourth Eighteenth Symposium (International) on Combustion*, 1992, pp. 213–221.

[7]Cheatham, S. and Matalon, M., "A General Asymptotic Theory of Diffusion Flames with Application to Cellular Instabilities," *Journal of Fluid Mechanics*, Vol. 414, 2000, pp. 105–144.

[8]Kukuck, S. and Matalon, M., "The Onset of Oscillations in Diffusion Flames," *Combustion Theory and Modelling*, Vol. 5, 2001, pp. 217–240.

[9]Pellet, G. L., Isaac, K. M., Humphreys, W. M. J., Gartrell, L. R., Roberts, W. L., Dancey, C. L., and Northam, G. B., "Velocity and Thermal Structure, and Strain-Induced Extinction of 14 to 100% Hydrogen-Air Counterflow Diffusion Flames," *Combustion and Flame*, Vol. 112, 2002, pp. 575–592.

[10]Frouzakis, C. E., Tomboulides, A. G., Lee, J., and Boulouchos, K., "From Diffusion to Premixed Flames in an H2/Air Opposed-Jet Burner: The Role of Edge Flames," *Combustion and Flame*, Vol. 130, 2002, pp. 171–184.

[11]Lu, Z. and Ghoshal, S., "Flame Holes and Flame Disks on the Surface of a Diffusion Flame," *Journal of Fluid Mechanics*, Vol. 513, 2004, pp. 287–307.

[12]Buckmaster, J. D. and Jackson, T. L., "Holes in Flames, Flame Isolas, and Flame Edges," *Proceedings of the Combustion Institute*, Vol. 28, 2000, pp. 1957–1964.

[13]Short, M. and Liu, Y., "Edge-flame Structure and Oscillations for Unit Lewis Numbers in a Non-premixed Counterflow," *Combustion Theory and Modelling*, Vol. 8, 2004, pp. 425–447.

[14]Margolis, B. S., "Bifurcation Phenomena in Burner-Stabilized Premixd Flames," *Combustion Science and Technology*, Vol. 22, 1979, pp. 143–169.

[15]Buckmaster, J. D., "Stability of the Porous Plug Burner Flame," *SIAM Journal on Applied Matematics*, Vol. 43, 6, 1983, pp. 1335–1349.

[16]Asher, U., Christiansen, J., and Russel, R. D., "Collocation Software for Boundary Value ODEs," *ACM Transactions on Math Software*, Vol. 7, 1981, pp. 223–229.

[17]Carpenter, M. H. and Kennedy, C. A., "Fourth-order 2N Storage Runge-Kutta Schemes," *NASA Technical Memorandum 109112*, 1994.

[18]Favier, V. and Vervisch, L., "Edge Flames and Partially Premixed Combustion in Diffusion Flame Quenching," *Combustion and Flame*, Vol. 125, 2001, pp. 788–803.